UCRL-JC-129417
PREPRINT

Modeling the Effect of Heatsink Performance in High-Peak-Power Laser-Diode-Bar Pump Sources for Solid-State Lasers

E. C. Honea, J. A. Skidmore, B. L. Freitas,
E. Utterback, M. A. Emanuel

This paper was prepared for submittal to the
SPIE Photonics West Conference
San Jose, CA
January 24-30, 1998

January 14, 1998

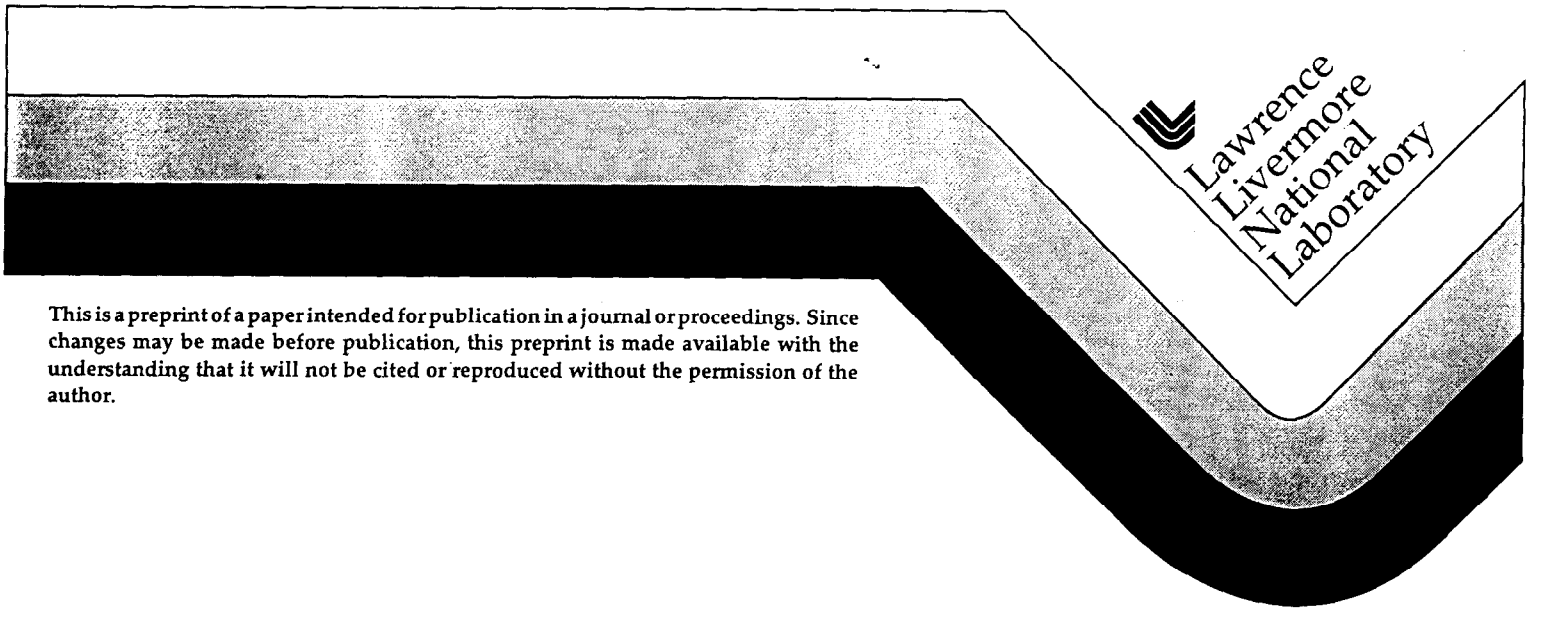

Modeling the effect of heatsink performance in high-peak-power laser-diode-bar pump sources for solid-state lasers

Eric C. Honea, Jay A. Skidmore, Barry L. Freitas,
Everett Utterback and Mark A. Emanuel

Lawrence Livermore National Laboratory, P.O. Box 808,
L-441, Livermore, CA 94551

ABSTRACT

We derive approximate expressions for transient output power and wavelength chirp of high-peak-power laser-diode bars assuming one-dimensional heat flow and linear temperature dependences for chirp and efficiency. The model is derived for pulse durations, $10 < \tau < 1000$ μs, typically used for diode-pumped solid-state lasers and is in good agreement with experimental data for Si heatsink mounted 940 nm laser-diode bars operating at 100 W/cm. The analytic expressions are more flexible and easily used than the results of operating point dependent numerical modeling. In addition, the analytic expressions used here can be integrated to describe the energy per unit wavelength for a given pulse duration, initial emission bandwidth and heatsink material. We find that the figure-of-merit for a heatsink material in this application is $(\rho C_p K)^{1/2}$ where ρC_p is the volumetric heat capacity and K is the thermal conductivity. As an example of the utility of the derived expressions, we determine an effective absorption coefficient as a function of pump pulse duration for a diode-pumped solid-state laser utilizing $Yb:Sr_5(PO_4)_3F$ (Yb:S-FAP) as the gain medium.

INTRODUCTION

As semiconductor-laser-diode technology progresses and output powers climb, heatsink performance plays an increasingly critical role in the overall system performance due to parasitic thermal effects which give rise to wavelength chirp and power sag (droop) during the pulse. One application of high-peak-power laser-diode bars utilizes a solid-state laser material such as $Nd:Y_3Al_5O_{12}$ (Nd:YAG) as an energy storage medium to produce very high peak power and brightness radiation. For these diode-pumped solid-state laser (DPSSL) systems the diode pump pulse duration is typically on the order of the solid-state laser upper lifetime, e.g. 230 μs for Nd:YAG. Since many solid-state laser materials such as Nd:YAG have absorption features only a few nanometers in width, efficient operation requires a correspondingly narrow diode emission,

including the effects of wavelength chirp. Furthermore, power sag over the course of the pulse affects the amount of total energy delivered during the diode pulse.

Advanced laser materials such as $Yb:Sr_5(PO_4)_3F$ (Yb:S-FAP) with lifetimes on the order of 1 ms have been developed in recent years to allow reduced diode power, thereby reducing cost, for a given output pulse energy.[1] However, this increased pulse duration exacerbates the effects of diode emission chirp and power sag. Therefore a detailed understanding of diode emission as a function of heatsink performance is required in order to maximize system performance and minimize cost.

Here we describe an approximate, analytical model of diode emission which assumes one-dimensional heat flow and linear temperature dependences for chirp and electrical efficiency. Unlike numerical methods,[2] the analytical expressions make it possible to quickly trade-off system parameters such as maximum output power, pulse duration, diode cavity length, maximum junction temperature rise and emission bandwidth tolerances. Good agreement is found between the model and experimental data from laser-diode bars mounted on Si heatsinks. Other heatsink materials are examined and a figure of merit is assigned based on their material thermal properties. As an example of the utility of the derived expressions, we determine an effective absorption coefficient as a function of pump pulse duration for a diode-pumped solid-state laser utilizing Yb:S-FAP as the gain medium.

DESCRIPTION OF MODEL

Figure 1 shows a cross-sectional view of a heatsink with a mounted laser bar. The figure is roughly drawn to scale showing typical values for cavity length (500 μm) and thickness (100 μm) of the GaAs diode bar. The laser bar is nominally 1 cm long, perpindicular to the plane of the drawing. We assume that heat is produced at the heatsink/GaAs interface since the active layer of the laser (where the heat is generated) is located within ~ 2 μm of that interface. Lateral temperature differences which may arise from the finite packing density of emitters as well as heat spreading at the bar ends are neglected. The thermal resistance of the metal/solder layers is also ignored because their thickness is much smaller than the nominal thermal diffusion lengths. The calculations assume that for the pulse durations of interest, the heat flow is one-dimensional into both the GaAs substrate and the heatsink material. This is a reasonable approximation since the diffusion length is less than the spacing between diode bars and comparable to or less than the cavity length for the pulse widths under consideration.

The thermal flux at the interface is given by $F=(1-\eta)P_{tot}/A$, where η is the electrical-optical efficiency of the laser-diode bar (and not the system wall-plug efficiency which also includes electrical contacts), P_{tot} is the electrical input power and $A=l_{cav}l_{bar}$ is the thermal footprint. Note

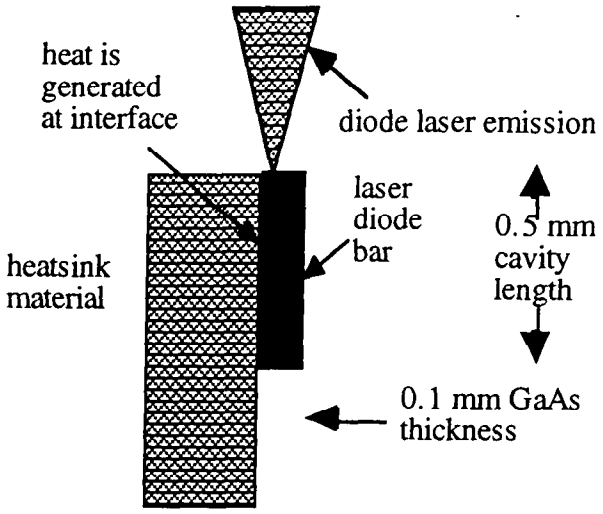

Figure 1: Schematic drawing of a laser-diode bar mounted on a heatsink.

that the heat is assumed to be dissipated uniformly across l_{bar}. This approximation is reasonably good for high-peak-power applications utilizing high-fill-factor bars (typically 0.70<ff<0.90) since the separation between emitters is small (~ 10 to 50 μm) compared to the thermal diffusion lengths of interest. For these calculations we take typical values for the cavity length, l_{cav}=500 μm and the bar length, l_{bar}=1 cm. In terms of the initial optical power, $P_{opt}=\eta_o P_{tot}$, the thermal flux is $(P_{opt}/A)(1-\eta_o)/\eta_o$. The electrical efficiency of the diode bar is a function of temperature, and as it heats up during a pulse, the optical output power will decrease although the total electrical power input remains constant. Since the reduction in efficiency feeds back additional heat to the diode, a "thermal runaway" is created.

We assume that for small temperature changes, the efficiency can be described by $\eta=\eta_o(1-\xi T)$ where T is the temperature rise, η_o is the optical efficiency at T=0 and ξ is the change in efficiency per unit temperature. Measurements of InAlGaAs diode performance over a narrow temperature range showed a decrease in output power of ~ 1%/°C.[3] Note that some designs and compositions are more temperature sensitive, so the sag could be greater.

The differential equations which describe the problem are then

$$\frac{\partial T}{\partial t} = \kappa \frac{\partial^2 T}{\partial x^2}$$

and

$$-K\frac{\partial T}{\partial x} = F = \frac{P_{opt}(1-\eta)}{A\eta} \approx \frac{P_{opt}}{A\eta_0}(1-\eta_0) + \frac{P_{opt}}{A}\xi T \quad \text{at } x = 0.$$

where K is the thermal conductivity, and κ is the thermal diffusivity

$$\kappa = \frac{K}{\rho C_p}.$$

For a single semi-infinite solid the solution is:[4]

$$T(x,t) = \left(\frac{\eta_0 - 1}{\xi\eta_0}\right)\left\{\operatorname{erfc}\left(\frac{x}{2\sqrt{\kappa t}}\right) - \exp\left[\frac{-P_{opt}\xi}{KA}x + \left(\frac{P_{opt}\xi}{KA}\right)^2 \kappa t\right]\operatorname{erfc}\left[\frac{x}{2\sqrt{\kappa t}} - \left(\frac{P_{opt}\xi}{KA}\right)\sqrt{\kappa t}\right]\right\}.$$

The temperature at the surface (x=0), which we take here as the laser-diode junction temperature, is therefore

$$T(x=0,t) = \left(\frac{\eta_0 - 1}{\xi\eta_0}\right)\left\{1 - \exp\left[\left(\frac{P_{opt}\xi}{KA}\right)^2 \kappa t\right]\operatorname{erfc}\left[\left(\frac{P_{opt}\xi}{KA}\right)\sqrt{\kappa t}\right]\right\}. \quad (1)$$

This equation is greatly simplified in the limit of ξ->0, reducing to

$$T(x=0,t) = \frac{2(1-\eta_0)P_{opt}}{\eta_0 KA}\sqrt{\frac{\kappa t}{\pi}}. \quad (2)$$

With these assumptions, the temperature increases with the square root of time, and at a given time is inversely proportional to $(\rho C_p K)^{1/2}$ which we take as the figure of merit (FOM) for a heatsink material. Since the heat flux is inversely proportional to the thermal footprint, we see that the diode cavity length, an important parameter that affects output performance and cost, also impacts the temperature rise for a given heatsink.

Equation 1 describes heat flow into a single semi-infinite material, however, some heat flows into the GaAs diode bar during the pulse creating a "thermal divider." We can account for this additional heat flow path by making the substitution[5]

$$\frac{\sqrt{\kappa}}{K} \rightarrow \frac{\sqrt{\kappa_{hs}\kappa_{GaAs}}}{K_{hs}\kappa_{GaAs}^{1/2} + K_{GaAs}\kappa_{hs}^{1/2}} \quad (3)$$

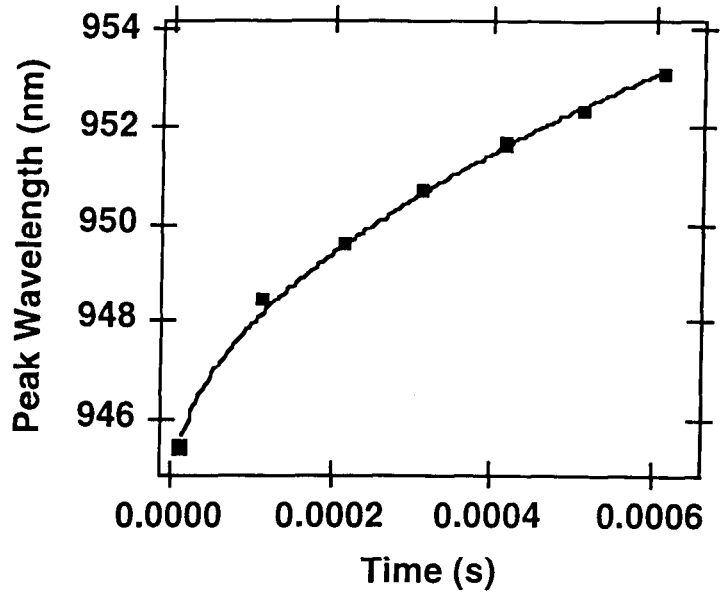

Figure 2: Measured values of peak wavelength (symbols) for a 940 nm diode array operated at 100 W/bar mounted onto a Si heatsink compared to model prediction. The solid line is a best fit to the data to determine the electrical efficiency, η=0.46, assuming a value of $d\lambda/dT$=0.35 nm/degree C.

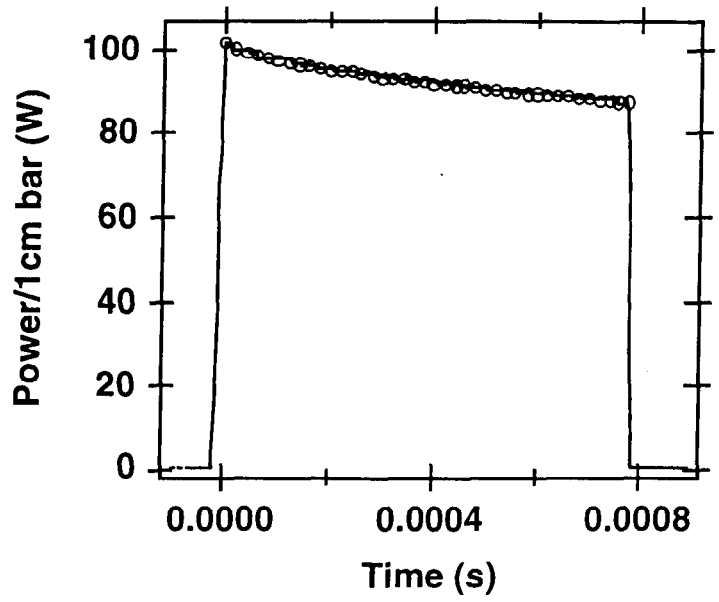

Figure 3: Measured power for a 940 nm array operated at 100 W/bar mounted onto a Si heatsink (solid line) compared to model prediction (symbols). Using the value of η=0.46 determined from the data in Figure 2, we obtain a value of dP/dT = 0.5 %/degree C.

The next parameter of interest is the effective emission bandwidth integrated over the entire pulse width including chirp and sag. To model this, we assume the power produced by the laser-diode bar is a gaussian with a full width half maximum of $\Delta\lambda$=1.665a, with a temperature dependent center wavelength, $\lambda_0(T)$ and power, P(T).

$$P(\lambda, T) = \frac{P(T)}{a\sqrt{\pi}} e^{-\left\{\frac{\lambda-\lambda_0(T)}{a}\right\}^2} \tag{4}$$

The gaussian is normalized such that the integral of the power over all wavelengths is 100 W. P(T) and $\lambda_0(T)$ are approximated by the linear functions described above. The energy as a function of wavelength in a pulse of width τ is therefore given by

$$E(\lambda, \tau) = \int_0^{\tau} P(\lambda, T(t))dt$$

where the time dependence of T has been explicitly noted. Assuming the gaussian initial emission spectrum and $T=b\sqrt{t}$ (i.e. equations (2) and (3) with the prefactor replaced by the single constant, b), this integral can be evaluated symbolically:

$$E(\lambda,\tau) = -\frac{aP_{opt}}{b^2\frac{d\lambda}{dT}}\left\{[-\tfrac{d\lambda}{dT}+\tfrac{dP}{dT}(\lambda-\lambda_0)]e^{-(\lambda-\lambda_0)^2/a^2} + 2a[-\tfrac{d\lambda}{dT}+\tfrac{dP}{dT}(\lambda-\lambda_0+b\tfrac{d\lambda}{dT}\sqrt{\tau})]e^{-\left(\lambda-\lambda_0-b\frac{d\lambda}{dT}\sqrt{\tau}\right)^2/a^2}\right\}$$
$$+\frac{P_{opt}}{2b^2\frac{d\lambda}{dT}}\left[\mathrm{erf}\left(\frac{\lambda-\lambda_0-b\frac{d\lambda}{dT}\sqrt{\tau}}{a}\right)-\mathrm{erf}\left(\frac{\lambda-\lambda_0}{a}\right)\right]\left[a^2\tfrac{dP}{dT}-2(\lambda-\lambda_0)\tfrac{d\lambda}{dT}+2(\lambda-\lambda_0)^2\tfrac{dP}{dT}\right]$$

From a perspective of designing the solid-state laser, it is the spectral integrated energy that matters. As shown in Figure 4, excellent agreement is found between predicted and measured values for various pulse widths (0.1, 0.2, 0.4 and 0.8 ms). This data is obtained using the efficiency value from Fig. 2 along with the dP/dT data from Fig. 3. The only remaining adjustable parameter is the initial width of the gaussian, a, in equation (4). The value used in the model predictions is a=2.3 nm corresponding to a FWHM of 3.8 nm.

FIGURE-OF-MERIT FOR HEATSINK MATERIALS

We can compare the predicted performance of several materials using the above equations. Since each heatsink material has certain cost and fabrication issues associated with it, the model provides a basis to determine cost/performance tradeoffs. Table I shows material properties, figure

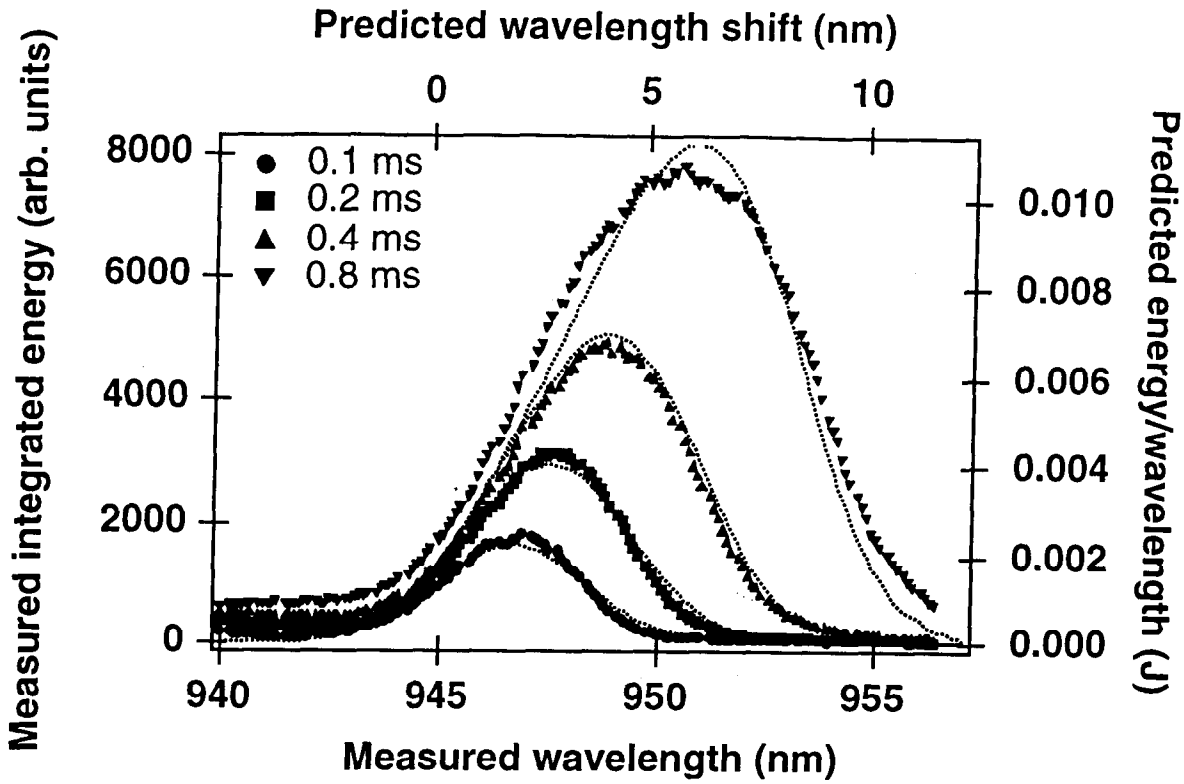

Figure 4: Measured integrated energy vs wavelength (symbols) for the 100 W/bar 940 nm array mounted on a Si heatsink compared to calculations (dotted line) using the parameters determined from Figures 3 and 4. The initial width of the gaussian (i.e. from center wavelength fabrication tolerances) is the only remaining parameter adjusted to match the data.

of merit (FOM), thermal diffusion length and predicted temperature rise for a 0.4 ms heat pulse assuming heat flow only into the heatsink and into both the GaAs and the heatsink.

The list of materials in Table I includes Si and BeO, which are believed to be most promising for these applications, as well as diamond (polycrystalline grown) and copper, which are examples of higher performance materials. Although the FOM for Si is only slightly greater than that of GaAs, the large technological base in Si processing and microtechnology may lead to cost advantages which outweigh thermal performance. Diamond offers the highest FOM, but at the present time material and fabrication costs are prohibitively expensive for large-scale heatsinks. Copper offers excellent thermal performance, however, the large thermal expansion mismatch may lead to problems of stress and unreliable contacts. Copper is oftentimes replaced by copper alloys (such as Cu-W or Cu-Mo) in order to provide thermal-expansion matching to GaAs, at the expense of reducing the thermal conductivity. Therefore we have also included a 10% Cu/ 90% W alloy in the table for comparison.

Table I: Material properties, figure of merit (FOM), thermal diffusion length L_d, and temperature rise at 0.4 ms predicted for one-dimensional heat flow with a heat flux of 2000 W/cm^2 at the surface. The thermal expansion coefficient, α, is included since mismatch between the heatsink and the GaAs diode bar may degrade reliability.

heat sink	K W/cm-°C	C_p J/gm-°C	ρ g/cm^3	α 10^{-6}/°C	FOM	L_d (0.4 ms)	ΔT (0.4 ms) heatsink only	ΔT (0.4 ms) heatsink and GaAs
diamond	14.0	0.472	3.51	1.2	4.82	581 µm	9.4	7.8
copper	4.0	0.390	8.96	16.6	3.74	214 µm	12.1	9.5
BeO	2.6	0.960	3.00	7.6	2.74	190 µm	16.5	12.1
10Cu/90W	2.05	0.160	17.0	6.5	2.36	174 µm	19.1	13.4
Si	1.48	0.720	2.33	3.0	1.58	188 µm	28.6	17.5
GaAs	0.54	0.350	5.32	6.0	1.00	108 µm	45.0	22.5

IMPACT OF DIODE HEATSINK PERFORMANCE ON ABSORPTION IN A Yb:S-FAP DPSSL

From the previous discussion we see that the diode emission width and energy depend on a number of parameters, including the pulse duration and heatsink material. For diode-pumped solid-state laser applications, the system design depends critically on the diode energy absorbed by the gain medium. An approximation to include the effects of the diode emission bandwidth and chirp is to calculate an effective unsaturated absorption cross section from the convolution with the absorption spectrum of the gain medium. With the present model, it is possible to calculate this cross-section for various heatsink materials and pump pulse durations. As an example, we calculate effective absorption cross sections for Yb:S-FAP as a function of pump pulse duration for values around the excited state lifetime of 1.1 ms. Since diode-pumped systems to date have utilized ~900 nm pumping for this material, the calculations were performed assuming a value of $d\lambda/dT$=0.32 nm/°C (estimated for ~ 900 nm emission[9]).

Figure 5 shows predicted energy vs wavelength for several heatsink materials assuming 100 W/cm, a pulse duration of 1 ms, a constant efficiency of 0.42 and dP/dT=0.01. Here we have assumed a FWHM of the diode emission of 8 nm at t=0 to reflect a plausible bandwidth for a large array. Although the peak of the emission shifts significantly, we see that the increase in width due to accumulated chirp is less than the initial width. In passing, we note that if a very small initial width is assumed the model predicts a pulse shape approaching that of a right triangle. This pulse

shape has appeared in previous reports[10] where the emission rises approximately linearly from the t=0 wavelength to a maximum corresponding to the wavelength at the end of the pulse and then drops abruptly.

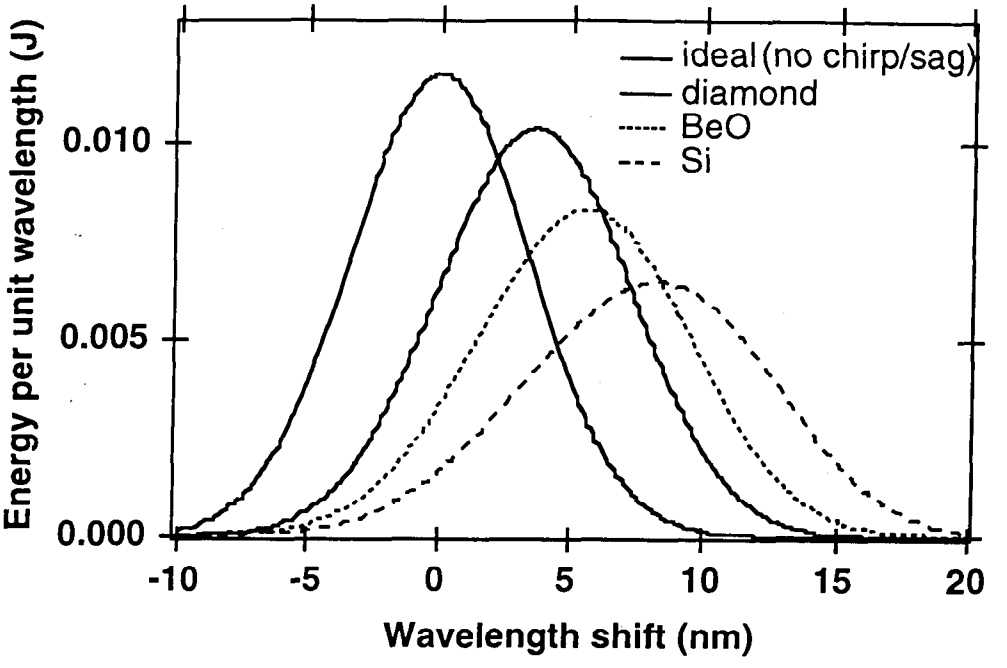

Figure 5: Predicted integrated energy vs wavelength for several heatsink materials assuming an initial width (t=0) of 8 nm FWHM, $d\lambda/dT$=0.32 nm/°C, an efficiency of 0.42, 1 ms pulse duration and an initial power of 100 W/cm.

Figure 6 shows the predicted diode emission curves for Si from Figure 5 overlaid with the small-signal transmission of a Yb:S-FAP crystal with a thickness of 4.2 cm and a Yb concentration of 2 x 10^{19} Yb/cm^3. The t=0 emission peak of the diode array has been shifted to 893 nm to optimize the pump absorption. From the Figure we see the diode emission is considerably wider than the wavelength range over which maximum absorption occurs, from ~899 - 903 nm.

We can calculate an effective absorption cross section for this pump duration and length/doping density product by calculating the transmission for the entire diode emission. Figure 7 shows a plot of effective absorption cross sections vs pump duration with the same parameters as those used for Figure 6. For each data point, the t=0 wavelength was optimized to obtain maximum absorption. Therefore, the data does not correspond to the case where a single array is operated at several pump pulse durations, but rather the optimum performance for a given pump pulse duration. The reduction in absorption cross section with increasing diode pulse width arises entirely from emission pulse shape. In addition to this effect, the average power emitted during the pulse decreases due to sag.

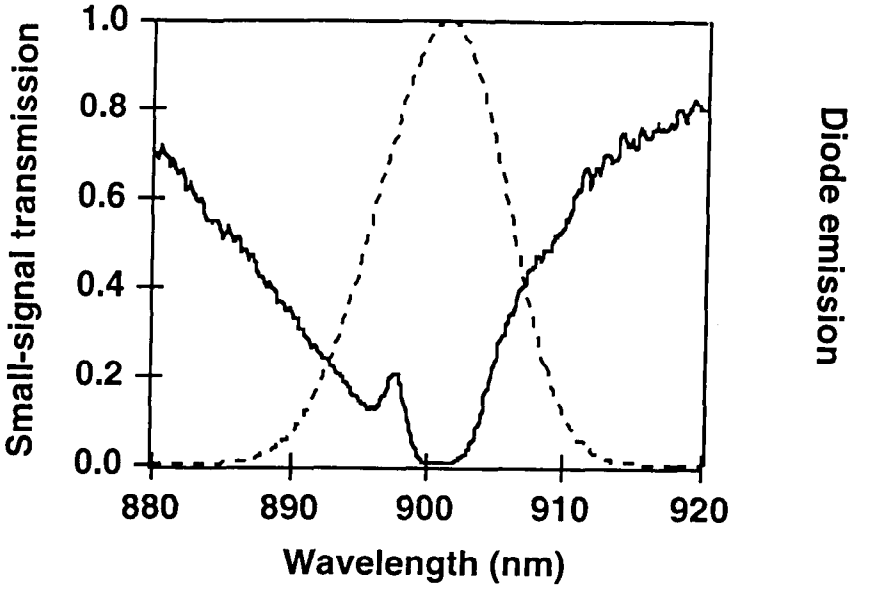

Figure 6: Predicted diode emission for 1 ms output, 100 W/cm diode bars mounted on Si and BeO heatsinks overlaid with the unsaturated transmission spectrum for a 4.2 cm thick S-FAP crystal with a Yb concentration of 2 x 10^{19} cm^{-3}.

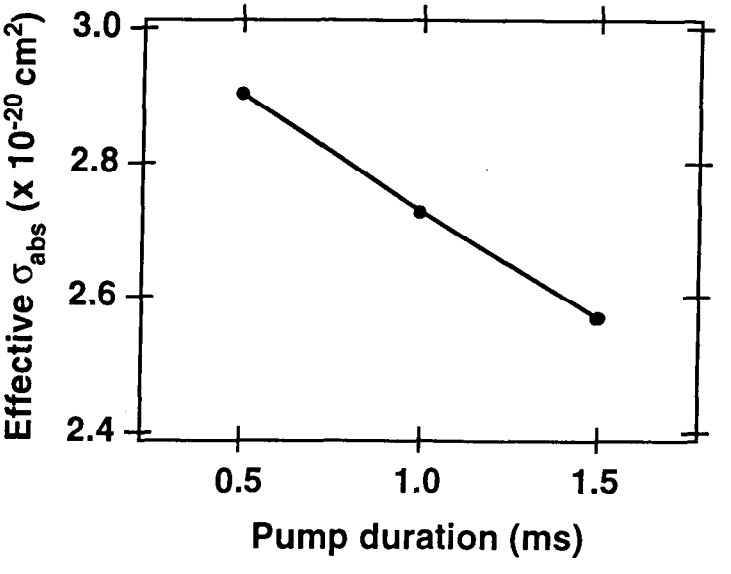

Figure 7: Predicted effective absorption cross section for a 4.2 cm thick S-FAP crystal with a Yb concentration of 2 x 10^{19} cm^{-3} using the same diode properties as those used in Figure 6.

CONCLUSIONS

We have derived a model to describe thermal effects in high-peak-power laser-diode bars. We find good agreement with measurements for 940 nm bars mounted on Si heatsinks. A figure-of-merit can be evaluated for prospective heatsink materials based on thermal conductivity and

volumetric heat capacity. The model yields analytic expressions which can be integrated into solid-state laser pump absorption modeling to determine the impact of these thermal effects on the solid-state laser performance. As an illustration of the utility of the model, we have calculated the effective absorption cross-section for a Yb:S-FAP laser utilizing 900 nm diode bars mounted on Si heatsinks.

ACKNOWLEDGEMENTS

This work was supported by the U.S. Department of Energy through the Lawrence Livermore National Laboratory under Contract W-7405-Eng-48.

REFERENCES

1. Stephen A. Payne, Laura D. DeLoach, Larry K. Smith, Wayne L. Kway, John B. Tossano and William F. Krupke, "Ytterbium-doped apatite-structure crystals: A new class of laser materials," J. Appl. Phys., 76, pp. 497-503, 1994. C. D. Marshall, L. K. Smith, R. J. Beach, M. A. Emanuel, K. I. Schaffers, J. Skidmore, S. A. Payne and B. H. T. Chai, "Diode-Pumped Ytterbium-Doped $Sr_5(PO_4)_3$ Laser Performance," IEEE J. Quantum Electron., 32, pp.650-656, 1996.

2. R. Puchert, M. Voss, Ch. Lier and A. Barwolff, "Transient temperature behavior of GaAlAs/GaAs-high power laser arrays on different heat sinks," SPIE Proceedings Vol. 2997, pp. 26-34, 1997.

4. Jay Skidmore, unpublished results.

5. "Conduction of Heat in Solids", H. S. Carslaw and J. C. Jaegar, Clarendon Press, Oxford, Second Edition, pp. 73-75.

6. ibid, p. 88.

6. M. A. Emanuel, J. A. Skidmore and R. J. Beach, "High-Power Laser Diodes at Various Wavelengths," SPIE Proceedings Vol. 3001, pp. 2-6, 1997.

7. M. Voss, C. Lier, U. Menzel, A. Barwollf and T. Elsaesser, "Time-resolved emission studies of GaAs/AlGaAs laser diode arrays on different heat sinks", J. Appl. Phys. 79, pp. 1170-1172, 1996.

8. H. I. Abdelkader, H. H. Hausien and J. D. Martin, "Temperature rise and thermal rise-time measurements of a semiconductor laser diode" Rev. Sci. Instrum. 63, pp. 2004-2007, 1992.

10. We take $d\lambda/dT$ to be proportional to λ^2 near room temperature.

10. R. Beach, W. J. Benett, B. L. Freitas, D. Mundinger, B. J. Comaskey, R. W. Solarz and M. A. Emanuel, "Modular Microchannel Cooled Heatsinks for High Average Power Applications", IEEE J. Quantum Electron., 28, pp. 966-976, 1992. J. G. Endriz, M. Vakili, G. S. Browder, M. DeVito, J. M. Haden, G. L. Harnagel, W. E. Plano, M. Sakamoto, D. F. Welch, S. Willing D. P. Worland and H. C. Yao, "High Power Diode Arrays", IEEE J. Quantum Electron., 28, pp. 952-965, 1992.

Technical Information Department • **Lawrence Livermore National Laboratory**
University of California • Livermore, California 94551